Electronic Supplementary Information (ESI) for Environmental Science: Nano

Sediments inhibit adsorption of 17β-estradiol and 17α-ethinylestradiol to carbon nanotubes and graphene oxide

Weiling Sun,[a,*] Menglin Li,[b] Wei Zhang,[c] Jingmiao Wei,[a] Ben Chen[d] and Conghe Wang[a]

[a] College of Environmental Sciences and Engineering, Peking University, The Key Laboratory of Water and Sediment Sciences, Ministry of Education, Beijing 100871, China

[b] Shenzhen Key Laboratory for Heavy Metal Pollution Control and Reutilization, School of Environment and Energy, Peking University Shenzhen Graduate School, Shenzhen 518055, China

[c] Department of Plant, Soil and Microbial Sciences; Environmental Science and Policy Program, Michigan State University, East Lansing, Michigan 48824, United States

[d] College of Resources Environment and Tourism, Capital Normal University, Beijing 100048, China

* Corresponding Author. Tel: +86-10-62756308

E-mail: wlsun@pku.edu.cn (Weiling Sun).

Text S1. Graphene oxide (GO) preparation

Four gram of graphite was added into 200 mL of cooled sulfuric acid (0–4 °C in an ice-bath). After stirring for 3 h at 0–4 °C, 24 g of $KMnO_4$ was slowly added into the mixture. After stirring for 4 h at 45 °C, 200 mL of deionized (DI) water was added. Meanwhile, the temperature was raised to 90 °C and then kept for 24 h. To stop the oxidation reaction, 300 mL hot DI water was added to the mixture. After 15 min, 40 mL H_2O_2 was added into the mixture. The supernatant was removed after centrifugation at 5000 rpm for30 min. The solid sample was washed with hydrochloric acid (5%, v/v) and DI water sequentially, and then freeze-dried. The GO suspension was then obtained by exfoliation of graphite oxide under ultrasonication for 12 h.

Text S2. Sediment preparation

The sediment sample was fractionated using the deposition method detailed by Dane and Topp.[S1] The method was based on the Stokes' law and assumed average particle density of 2.65 g/cm^3 and spherical particles. About 20-30 g of the < 63-μm sediments were placed into a 1-L beaker and dispersed with 1 L DI water, resulting in a sediment suspension of less than 3% by mass. The sediment suspension was stirred with a special blender to prevent vortex. The settling time for a given particle diameter to fall below certain depth was estimated according to the Stokes' law. After settling for pre-determined time, the suspension in the upper layer above certain depth containing the desired particle sizes was removed using a siphon pipe. When withdrawing the suspension, the siphon elbow was placed upward to avoid taking the lower suspension. The sedimentation procedure was repeated to separate five size fractions, namely, the colloid (< 1 μm),

clay (1–2 μm), fine silt (2–5 μm), small silt (5–10 μm), and large silt (10–63 μm) fractions. The suspensions were freeze-dried, and the various sediment size fractions were used in subsequent adsorption experiments.

Text S3. E2 and EE2 quantification

The E2 and EE2 concentrations were measured using a fluorescence quenching method by a fluorescence spectrophotometer (Cary Eclipse, Varian, USA) as previously described.[S2,S3] The excitation source was a 450-W xenon lamp with the slits set to 5 nm for both excitation (Ex) and emission (Em). The fluorescence intensity of E2 and EE2 was determined at 280 nm (Ex)/310 nm (Em) according to our previous studies.[S2,S3] The calibration curves included six concentration levels in the range of 0.02–2.4 mg L^{-1}, similar to the experimental conditions. The calibration curves were linear with correlation coefficient (R) greater than 0.999. The method detection limits (MDL) for E2 and EE2 were 12 and 13 μg L^{-1}, respectively. The fluorescence intensity of 0.01 M NaCl background solution were measured and subtracted.

Text S4. Density functional theory (DFT) calculation

The binding energies of E2 or EE2 with CNTs or GO were calculated using the DFTB+ code of Material Studio package (version 7.0). The Slater-Koster files from the well-established *mio* set were used. The self-consistent charges (SCC) calculation for periodic structures were performed with the SCC tolerance set to 10^{-5}. The smearing value was 0.005 Ha. The convergence thresholds were 0.05 kcal mol^{-1} (Energy) and 0.5 kcal mol^{-1} $Å^{-1}$ (Force).

In DFT calculation, it is important to select the size of CNTs. The use of the actual CNT size

was not possible due to unrealistic long computation time.[S4] Zhou et al.[S5] found that during DFT calculation the outer diameter of CNTs (D) should not be less than the distance of two outer hydrogen atoms in organic molecule (d). Otherwise, the calculated binding energies (E_{bd}) would change with D. Therefore, in this study the chiral vectors (n and m) were set to n = 12 and m = 12. That is, a series of (12,12) armchair structure containing 216 benzene rings were used as model CNTs. Both ends of the model CNTs were saturated by hydrogen atoms. Thus, the size of CNTs were 24.60 Å in length and 16.27 Å in D (Fig. S8a), which is greater than the d value of E2 (12.73 Å) and EE2 (14.46 Å) (Fig. S8c). Therefore, the calculated E_{bd} values would not be influenced by D. The GO structure was represented by a 11×11 supercell with the following unit cell parameters: $a = b$ = 29.52 Å, c = 10.00 Å; $\alpha = \beta$ =90°, γ =120° (Fig. S8b).[S6]

In the adsorption experiments, the carboxylated CNTs and GO were used as adsorbents. Moreover, the hydroxyl group (–OH) was the predominant functional group on the surface of GO according to the XPS analysis (Table S1). Therefore, carboxylated CNTs and hydroxylated graphene (GO) were used to simulate E2 or EE2 adsorption by CNMs. Additionally, only the dissociated –COOH group ($–COO^-$) was used in the calculation, because the hydrogen in carboxyl group on the surface of CNTs was dissociated at the experimental pH of 7.5 ± 0.2. The electronic state of COO^- was modeled as the spin-restricted singlet.[S7]

The binding energies (E_{bd}) were calculated via Eq. (1) to determine the most stable structures of E2 or EE2 with CNMs.

$$E_{bd} = E_A + E_B - E_{AB} \quad (1)$$

(A = E2 or EE2, B = CNTs or GO)

where E_{AB} is the total energy of the whole system, E_A is the energy of E2 or EE2, and E_B is the energy of CNTs or GO, respectively. The positive value of E_{bd} means the adsorption is an exothermic reaction with a higher value indicating a stronger binding.[S8]

Text S5. DLVO calculation

In this study, DLVO energy was estimated for CNMs interacting with sediment surface using the sphere-plate configuration, and for CNMs interacting with CNMs using the sphere-sphere configuration, respectively. The total DLVO interaction energy (Φ_{tot}) was calculated by Eq. (2):[S9]

$$\Phi_{tot} = \Phi_{vdw} + \Phi_{edl} \qquad (2)$$

where Φ_{vdw} is the van der Waals interaction energy, and Φ_{edl} is electrical double layer interaction energy.

(1) Sphere-sphere configuration

Φ_{vdw} can be written as:[S10,S11]

$$\Phi_{vdw} = -\frac{A_{131}}{6}\left[\frac{2r^2}{h^2+4rh} + \frac{2r^2}{h^2+4rh+4r^2} + \ln\left(\frac{h^2+4rh}{h^2+4rh+4r^2}\right)\right] \qquad (3)$$

where r is to the radius of CNM particle, h is the separation distance between CNMs and CNMs, and A_{131} is the Hamaker constant for the substance 1 in the presence of medium 3. A_{131} can be determined from the Hamaker constant of individual material.[S12,S13]

$$A_{131} = \left(\sqrt{A_{11}} - \sqrt{A_{33}}\right)^2 \qquad (4)$$

where A_{11} is the Hamaker constant for CNMs, A_{33} is the Hamaker constant for water (i.e., 3.7×10^{-20} J).[S14]

Φ_{edl} can be written as:[S11,S13]

$$\Phi_{edl} = 32\pi r\varepsilon_r\varepsilon_0\left[\frac{k_BT}{ze}\right]^2\tanh\left[\frac{ze\psi_{p_1}}{4k_BT}\right]\tanh\left[\frac{ze\psi_{p_1}}{4k_BT}\right]exp(-\kappa h) \quad (5)$$

$$\kappa^{-1} = \sqrt{\frac{\varepsilon_r\varepsilon_0k_BT}{2N_AIe^2}} \quad (6)$$

where ε_r is the dielectric constant of the medium (78.4 for water), ε_0 is the vacuum permittivity (8.854×10^{-12} C^2 N^{-1} m^{-2}), $k_B$is the Boltzmann constant (1.381×10^{-23} C^2 J K^{-1}), T is the temperature (298.15 K), z is the valence of electrolyte, e is the electron charge (1.602×10^{-19} C), ψ_{p1} is the surface potentials of CNMs, κ is the reciprocal of the Debye length, $N_A$is the Avogadro constant (6.02×10^{23} mol^{-1}), and I is solution ionic strength. The surface potential (ψ) of CNMs could be calculated from measured zeta potentials (ξ).[S15]

$$\psi = \xi\left(1+\frac{d}{r}\right)exp(\kappa d) \quad (7)$$

where d is the distance between the surface of the charged particle and the slipping plane, and usually taken as 5 Å.

(2) Sphere-plate configuration

Φ_{vdw} can be written as:[S11]

$$\Phi_{vdw} = -\frac{A_{132}}{6}\left[\frac{r}{h}+\frac{r}{h+2r}+ln\left(\frac{h}{h+2r}\right)\right] \quad (8)$$

A_{132} is the Hamaker constant for the substance 1 interacting with the substance 2 in the medium 3 (i.e., water). Again, A_{132} can be determined as follows.[S13]

$$A_{132} = \left(\sqrt{A_{11}}-\sqrt{A_{33}}\right)\left(\sqrt{A_{22}}-\sqrt{A_{33}}\right) \quad (9)$$

where A_{22} is the Hamaker constant for sediments.

Φ_{edl} can be written as:[S12,S13]

$$\Phi_{edl} = 64\pi r\varepsilon_r\varepsilon_0\left[\frac{k_BT}{ze}\right]^2 \tanh\left[\frac{ze\psi_p}{4k_BT}\right]\tanh\left[\frac{ze\psi_c}{4k_BT}\right]exp(-\kappa h) \quad (10)$$

where ψ_c is the surface potential of sediments.

The Hamaker constants of CNTs and sediments were calculated from Eq. (11).

$$A_L = 4A_S / (1+\cos\theta)^2 \quad (11)$$

where A_L is the Hamaker constant of liquid (i.e., 3.7×10^{-20} J for water), and A_s is the Hamaker constant of the material.[S16,S17]

Contact angles of CNTs and sediments with or without OM were measured by OCA2O (Dataphysics, Germany) against water after these materials were tableted. Sessile drop technique was used in contact angle measurements. The reported contact angles under all examined conditions were the average of 10 replicated measurements. The contact angles and the Hamaker constants of original sediments, OM-free sediments, and CNMs are shown in Table S7.

Table S1 Properties of CNMs.

CNMs	XPS (%)		O 1s		S_{BET} (m^2/g)	V_{micro} (10^{-3} cm^3/g)	Pore diameter (nm)
	C	O	O=C-O (%) 531.0 eV	O-C (%) 532.7 eV			
CNTs	94.8	5.2	41.9	58.1	156	944	24.3
GO	69.0	30.0	2.7	97.3	15.4	6	0.14

Table S2 Properties of untreated and OM-free sediments.

Sediment fraction	S_{BET} (m^2/g)	V_{micro} (10^{-3} cm^3/g)	Pore diameter (nm)	TOC (mg/g)	Dominant mineral type	Other minerals in all < 10 μm size fractions
Untreated sediments						
<1μm	25.1	116	18.4	19.7	Calcite, quartz, gypsum, gismondine	smectite, mica and/or illite chlorite, montmorillonite, kaolinite, hematite, plagioclase
1-2 μm	24.2	108	17.8	16.0	Quartz, gismondine, calcite	
2-5 μm	17.3	68	15.6	14.7	Quartz, gismondine	
5-10 μm	16.5	64	15.6	13.5	Quartz, gismondine	
10-63 μm	7.36	29	15.8	9.68	Quartz	
OM-free sediments						
<1μm	45.9	143.8	12.5			
1-2 μm	40.8	156.3	15.3			
2-5 μm	24.9	89.6	14.4			
5-10 μm	18.0	70.0	15.5			
10-63 μm	8.37	31.9	15.2			

Table S3 Adsorption parameters of E2 and EE2 by various sediment particle fractions[a].

Adsorbate	Sediments (μm)	Linear		K_{oc} (L/kg C)	S_{BET}-normalized K_d (L/m^2)
		K_d (L/g)	R^2		
E2	<1	0.980	0.986	4.97×10^4	0.039
	1-2	0.627	0.994	3.93×10^4	0.026
	2-5	0.522	0.991	3.55×10^4	0.030
	5-10	0.211	0.985	1.56×10^4	0.013
	10-63	0.174	0.944	1.80×10^4	0.024
EE2	<1	0.456	0.966	2.31×10^4	0.018
	1-2	0.200	0.946	1.25×10^4	0.008
	2-5	0.039	0.966	2.62×10^3	0.002
	5-10	0.022	0.979	1.62×10^3	0.001
	10-63	0.018	0.941	1.81×10^3	0.002

[a] The linear (Eq. (12)) model was applied to describe the adsorption isotherms:

Linear isotherm: $Q_e=K_d\cdot C_e$ (12)

where Q_e (mg/g) is the equilibrium adsorption amount, C_e (mg/L) is the aqueous equilibrium concentration of E2 or EE2, K_d (L/g) is the distribution coefficient.

142 **Table S4** Fitting results of E2 and EE2 adsorption isotherms on CNTs and GO alone and their mixtures with sediments.

Adsorbate	Adsorbent	Linear		Langmuir[a]			Freundlich[b]			$K_{d,0.5}$[d]
		K_d (L/g)	R^2	Q_m	b	R^2	K_f[c]	1/n	R^2	(L/g)
E2	CNTs	58.1	-0.044	37.0	10.0	0.992	41.0	0.395	0.987	62.4
	CNTs+1	27.0	0.93	55.6	0.811	0.913	25.4	0.728	0.996	30.7
	CNTs+2	23.1	0.525	29.3	2.82	0.936	21.1	0.408	0.964	31.8
	CNTs+5	35.3	0.345	31.9	5.71	0.948	27.7	0.349	0.978	43.5
	CNTs+10	46.6	0.445	36.9	5.53	0.956	33.8	0.403	0.984	51.1
	CNTs+63	51.2	0.000	36.1	8.66	0.995	38.5	0.409	0.982	58.0
EE2	CNTs	43.0	-0.142	33.6	8.28	0.984	33.9	0.383	0.969	52.0
	CNTs+1	12.9	0.416	21.2	2.14	0.912	14.2	0.784	0.983	16.5
	CNTs+2	13.6	0.811	33.8	0.744	0.836	14.1	0.677	0.966	17.6
	CNTs+5	25.3	0.284	27.9	4.32	0.957	22.5	0.353	0.982	35.2
	CNTs+10	23.7	0.173	27.0	4.25	0.961	22.2	0.395	0.975	33.8
	CNTs+63	27.1	0.280	30.8	3.53	0.987	25.2	0.471	0.971	36.4
E2	GO	454	0.908	96.2	8.00	0.832	246	0.750	0.959	293
	GO+1	18.9	0.870	33.9	1.161	0.844	18.0	0.604	0.980	23.7
	GO+2	20.6	0.291	24.6	3.658	0.953	19.4	0.407	0.982	29.3
	GO+5	22.8	-0.024	25.6	5.200	0.979	21.5	0.342	0.996	33.9
	GO+10	30.0	0.673	36.4	2.391	0.970	26.9	0.541	0.993	37.0
	GO+63	85.3	0.686	44.4	7.50	0.921	47.7	0.429	0.991	70.9
EE2	GO	355	0.936	74.63	9.571	0.798	160	0.658	0.985	203
	GO+1	7.76	0.980	42.74	0.240	0.563	8.07	0.803	0.981	9.25
	GO+2	9.89	0.714	23.81	0.897	0.975	10.9	0.645	0.971	13.9
	GO+5	11.3	-0.411	17.45	3.201	0.997	13.0	0.408	0.933	19.6
	GO+10	13.1	0.142	20.28	2.651	0.980	14.3	0.419	0.985	21.4
	GO+63	18.6	0.852	39.68	0.890	0.929	18.5	0.675	0.987	23.2

[a] Langmuir equation: $Q_e = \frac{Q_m \cdot b \cdot C_e}{1 + b \cdot C_e}$ (13)

[b] Freundlich equation: $Q_e = K_f \cdot C_e^{1/n}$ (14)

where Q_e (mg/g) is the adsorption amount after equilibrium, C_e (mg/L) is the aqueous equilibrium concentration of E2 or EE2, Q_m (mg/g) is the maximal adsorption capacity, b (L/mg) is the Langmuir constant, K_f ((mg/g)/(mg/L)$^{1/n}$) is the Freundlich distribution coefficient, and 1/n is the Freundlich empirical constant describing the degree of nonlinearity.

[c] The unit is (mg/g)/(mg/L)$^{1/n}$

[d] single point K_d values at E2/EE2 equilibrium concentration of 0.1 mg/L and 0.5 mg/L

Table S5 Calculated binding energies (E_{bd}) of CNMs-E2/EE2 complexes.

NMs	Pollutants	E_A[a]	E_B[a]	E_{AB}	E_{bd} (kcal/mol)
CNTs-COO$^-$[b]	E2	-29209.7	-537754.4	-567061.5	97.3
CNTs-COO$^-$	EE2	-31370.4	-537754.4	-569177.1	52.3
GO[c]	E2	-29209.7	-315785.4	-345139.3	144.1
GO	EE2	-31370.4	-315785.4	-347285.3	129.5

[a] A = E2 or EE2, B = CNT or GO

[b] CNTs with dissociated –COOH group

[c] Graphene with –OH group

Table S6 Fitting results of E2 and EE2 adsorption isotherms on CNTs or GO alone and their mixtures with OM-free sediment.

Adsorbate	Adsorbent	Linear		Langmuir			Freundlich			$K_{d,0.5}$
		K_d (L/g)	R^2	Q_m	b	R^2	K_f[a]	1/n	R^2	(L/g)
E2	CNTs	58.1	-0.044	37.0	10.0	0.992	41.0	0.395	0.966	62.4
	CNTs+1	24.5	-2.99	22.3	560	0.991	25.6	0.224	0.863	43.8
	CNTs+2	31.9	-0.782	27.5	14.6	0.988	26.8	0.245	0.993	45.2
	CNTs+5	32.0	-0.546	27.8	12.0	0.981	26.7	0.264	0.966	44.5
	CNTs+10	33.1	-0.642	29.2	9.53	0.989	29.4	0.356	0.921	45.9
	CNTs+63	36.6	-1.07	29.2	17.1	0.995	31.2	0.299	0.947	50.7
EE2	CNTs	43.0	-0.142	33.6	8.28	0.984	33.9	0.383	0.969	52.0
	CNTs+1	18.1	-1.85	20.1	45.2	0.999	20.3	0.198	0.955	35.4
	CNTs+2	18.5	-3.50	19.8	38.9	1.00	20.4	0.198	0.873	35.6
	CNTs+5	20.6	-2.44	21.5	22.2	1.00	21.6	0.232	0.932	36.8
	CNTs+10	21.4	-2.86	21.6	35.6	1.00	22.8	0.230	0.880	38.9
	CNTs+63	22.8	-2.04	22.5	23.4	0.995	23.4	0.264	0.917	39.0
E2	GO	454	0.908	96.2	8.00	0.832	246	0.750	0.959	293
	GO+1	15.1	-3.18	17.8	18.7	0.999	17.2	0.212	0.922	29.7
	GO+2	12.3	-4.63	14.6	24.4	1.00	14.2	0.184	0.913	25.0
	GO+5	13.2	-1.82	16.3	8.54	0.991	14.4	0.246	0.957	24.3
	GO+10	14.1	-3.82	17.0	19.6	0.999	16.2	0.182	0.954	28.6
	GO+63	17.6	-1.84	20.2	11.3	0.995	18.7	0.246	0.956	31.5
EE2	GO	355	0.936	74.6	9.57	0.798	160	0.658	0.985	203
	GO+1	11.8	-1.53	15.8	7.46	0.979	13.9	0.306	0.907	22.5
	GO+2	11.3	-1.23	15.2	5.66	0.977	12.8	0.305	0.934	20.7
	GO+5	10.0	-0.752	14.7	4.01	0.968	11.4	0.334	0.931	18.1
	GO+10	13.3	-0.862	18.3	4.88	0.994	15.1	0.356	0.932	23.6
	GO+63	14.0	-0.503	19.4	4.22	0.995	15.5	0.363	0.970	24.1

[a] $(mg/g)/(mg/L)^{1/n}$

Table S7 Contact angles and Hamaker constants of untreated sediments, OM-free sediments, and CNMs.

	Particle size (μm)	Contact angle (°)	Hamaker constant (J)
Untreated Sediments	<1	22.15	3.43E-20
	1-2	17.95	3.52E-20
	2-5	17.50	3.53E-20
	5-10	17.15	3.54E-20
	10-63	13.60	3.60E-20
OM-free sediments	<1	21.70	3.44E-20
	1-2	16.85	3.54E-20
	2-5	13.20	3.60E-20
	5-10	12.50	3.61E-20
	10-63	10.60	3.64E-20
CNTs		16.40	3.55E-20
GO		-	1.28E-20[15]

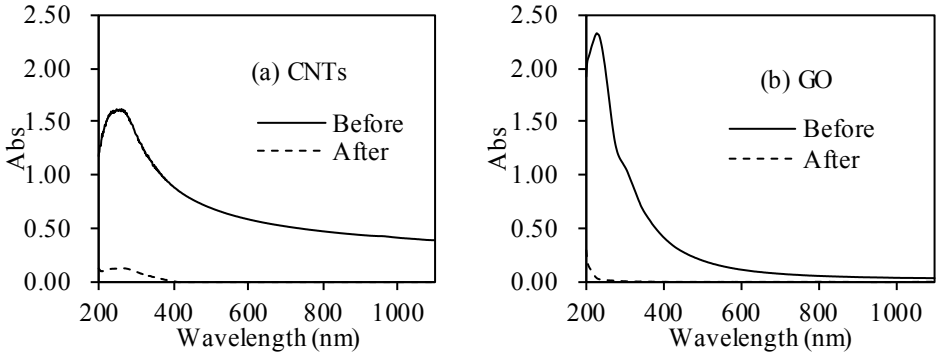

Fig. S1 The absorbance of CNTs or GO solution before and after centrifugation and filtration (ionic strength 0.01 M NaCl, CNMs concentration = 50 mg/L).

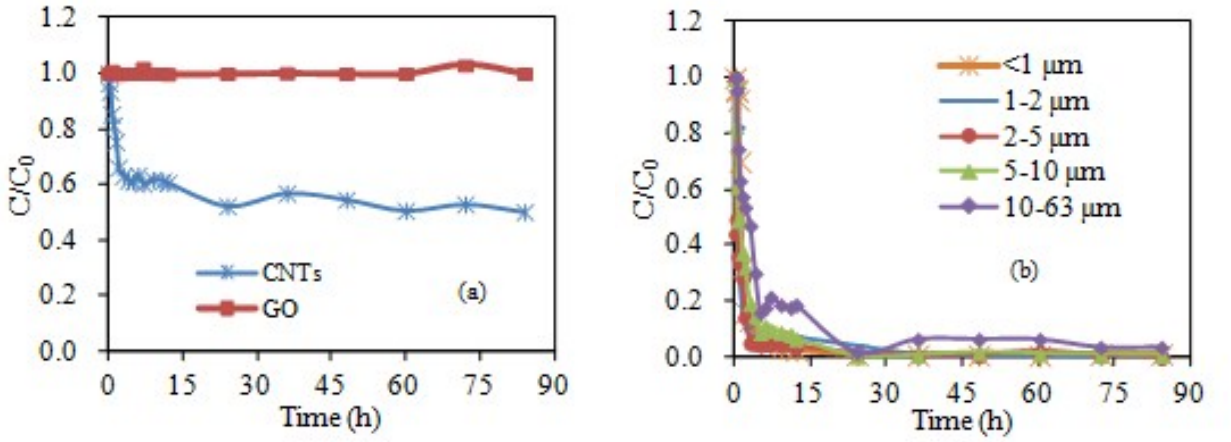

Fig. S2 Sedimentation kinetics of (a) CNMs and (b) sediments alone (Sediment = 500 mg/L, CNTs = 50 mg/L, ionic strength = 0.01 mol/L NaCl).

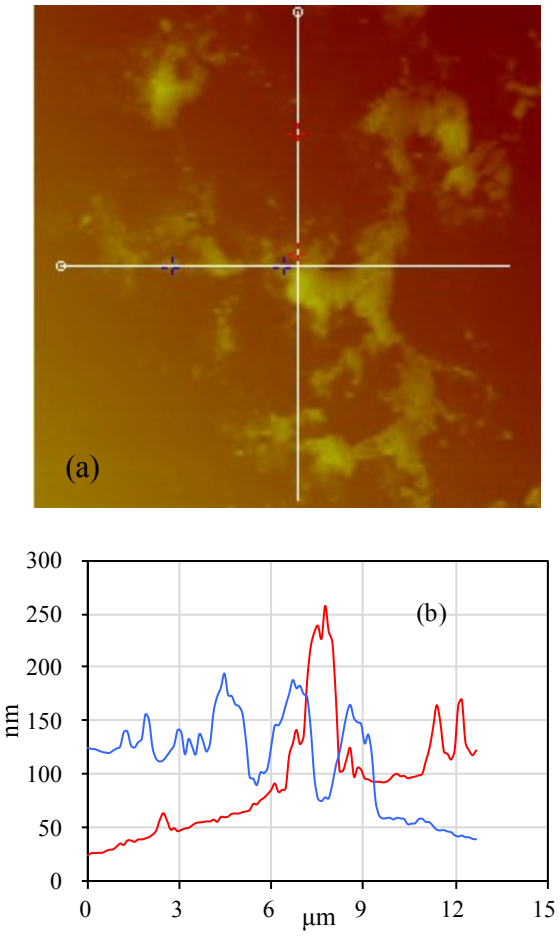

Fig. S3 AFM images of GO (a) and AFM height analysis (b).

173

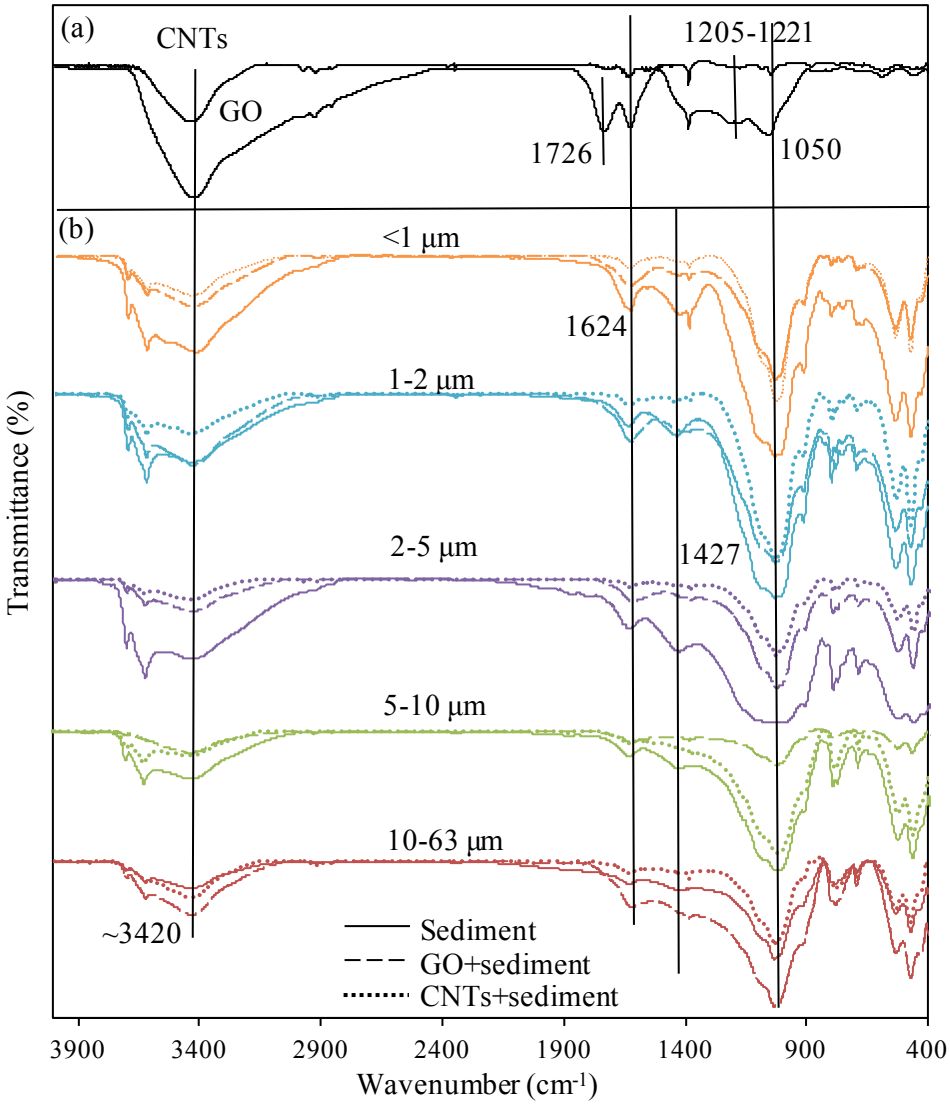

174

175 **Fig. S4** FTIR spectra of CNTs and GO (a), various sediment size fractions and their mixtures with

176 CNMs (b).

177

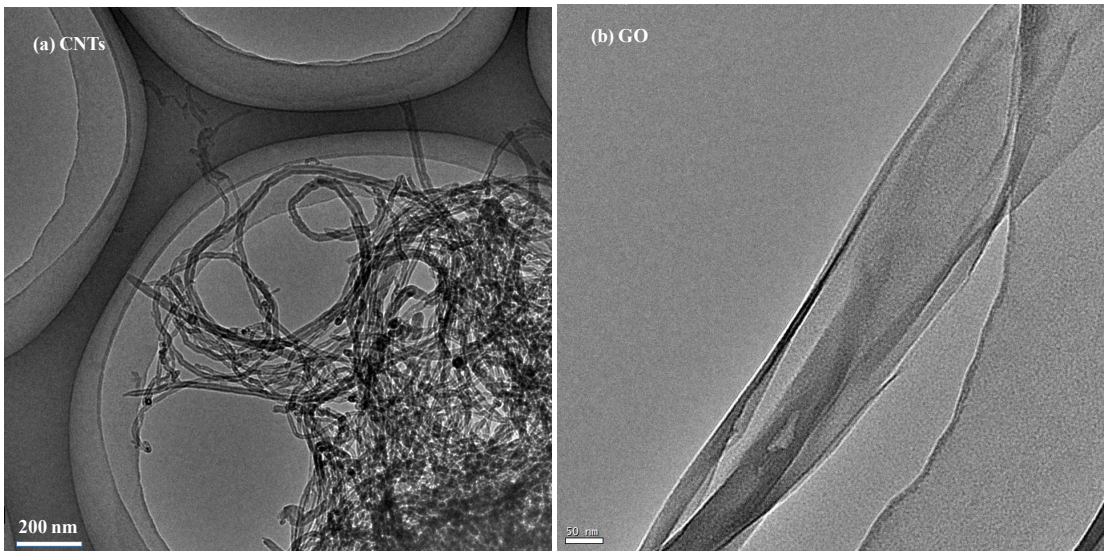

178

179 **Fig. S5** TEM images of CNTs (a) and GO (b).

180

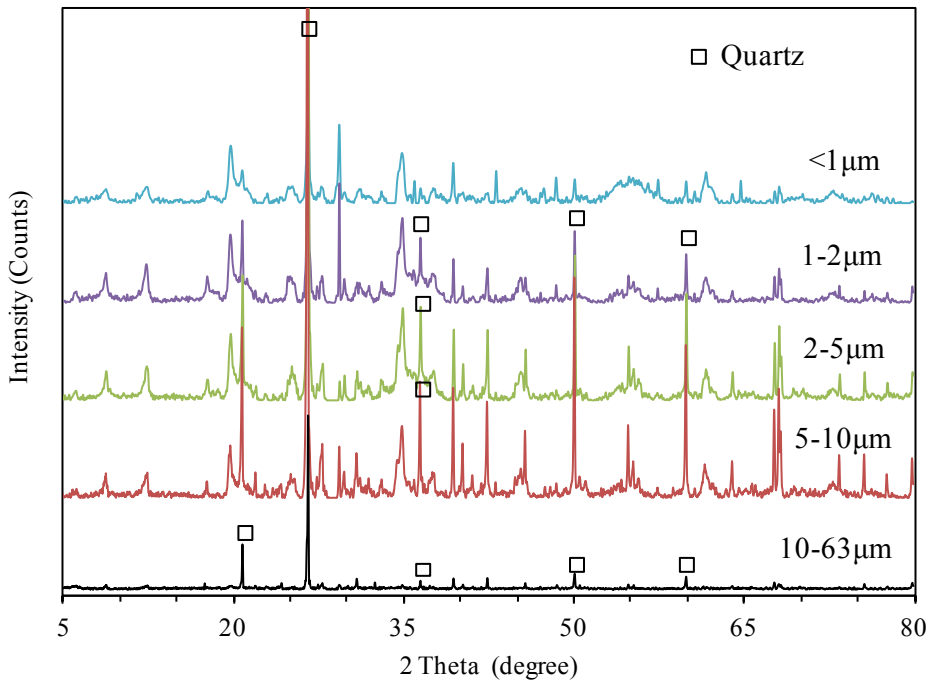

181

182 **Fig. S6** XRD patterns of various sediment size fractions.

183

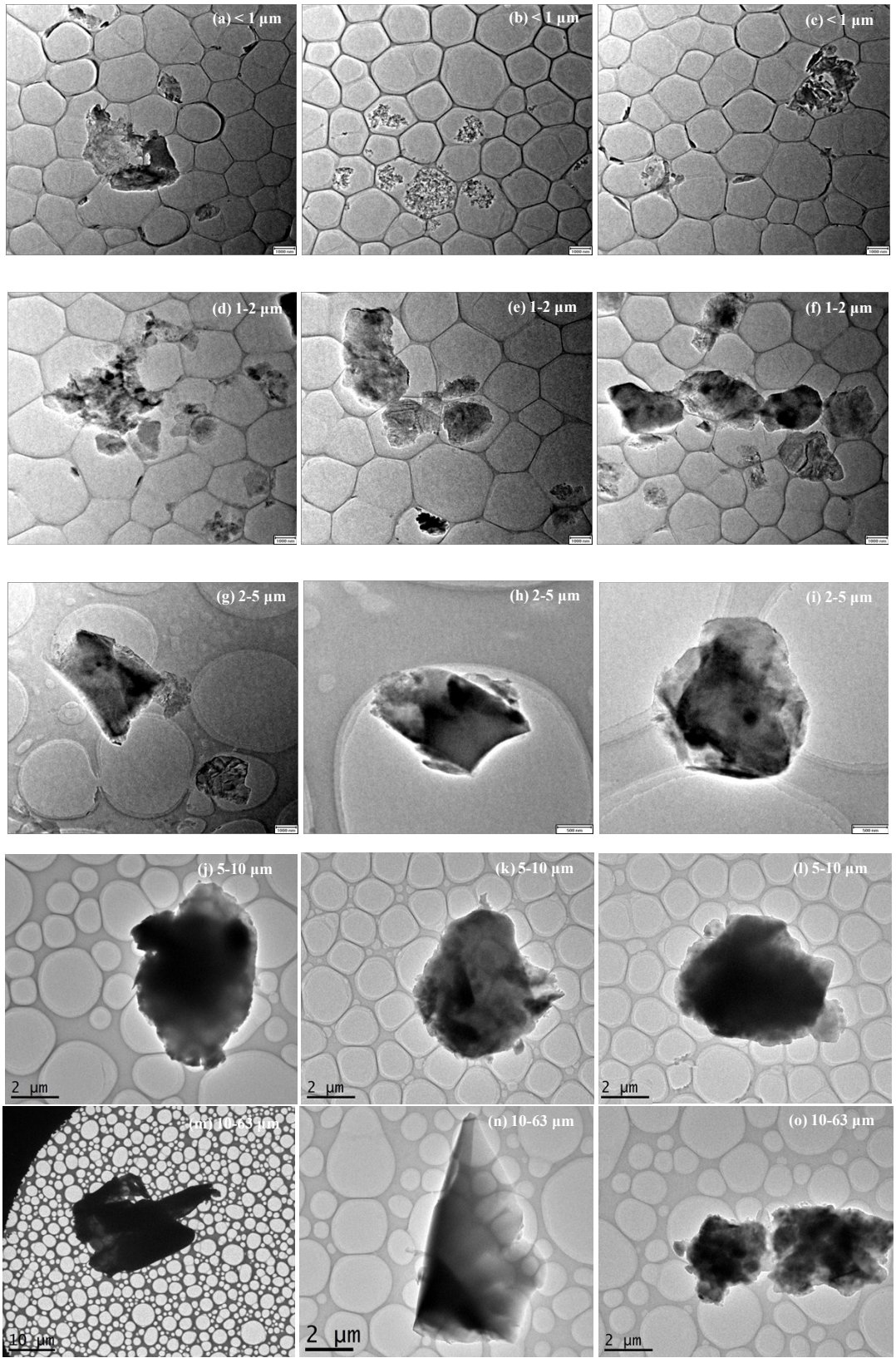

Fig. S7 TEM images of various sediment size factions.

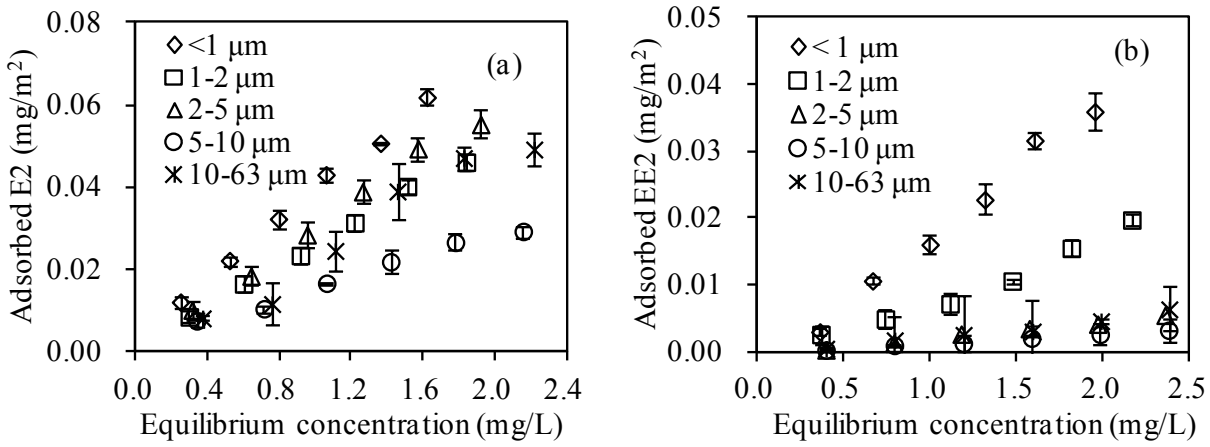

190

191 **Fig. S8** S_{BET}-normalized adsorption isotherms of E2 (a) and EE2 (b) by various sediment size

192 fractions.

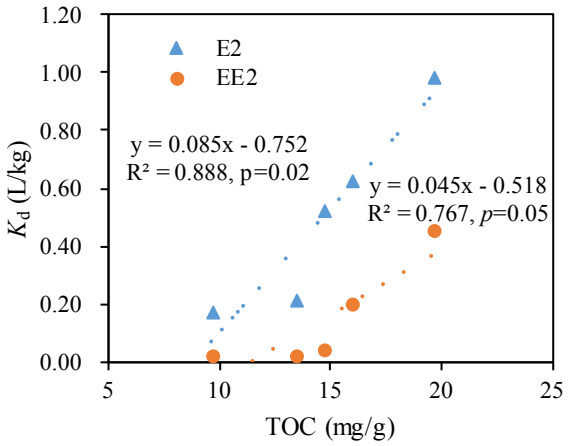

193

194 **Fig. S9** Correlation between sorption coefficients (K_d) of E2 and EE2 and TOC of various sediment

195 size fractions.

196

197

(a) CNTs-COO$^-$

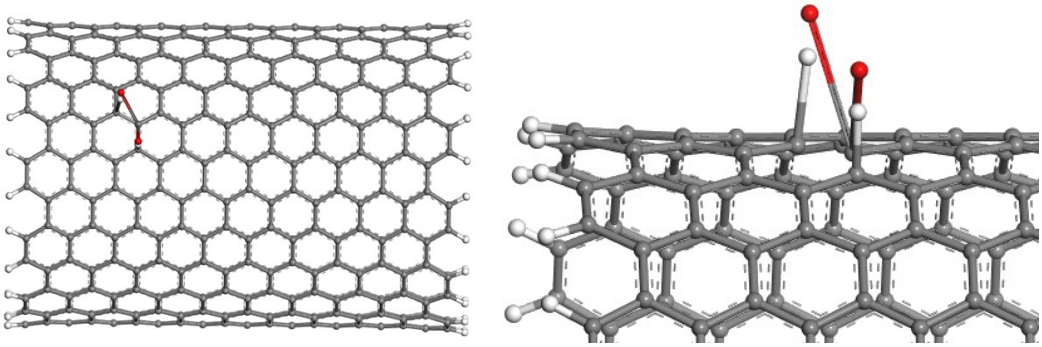

(b) GO

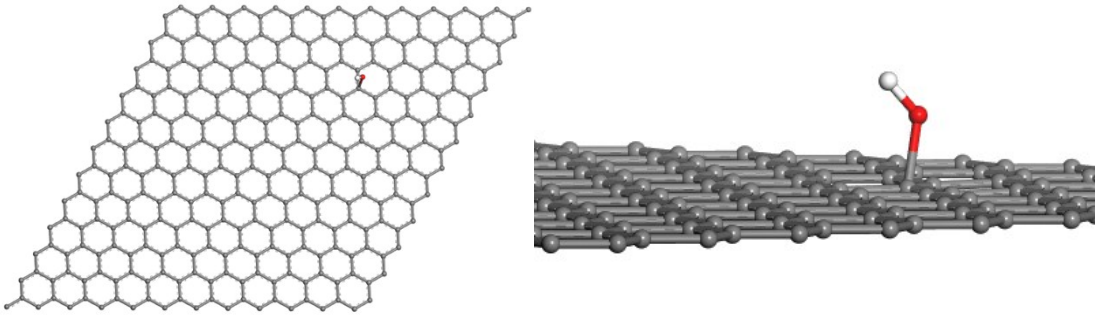

(c) E2 and EE2

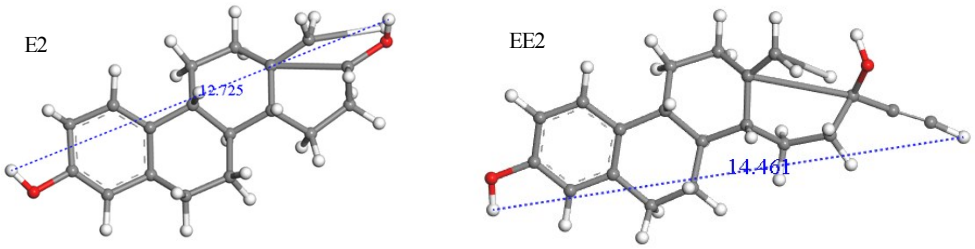

(d) CNTs-COO$^-$ + E2

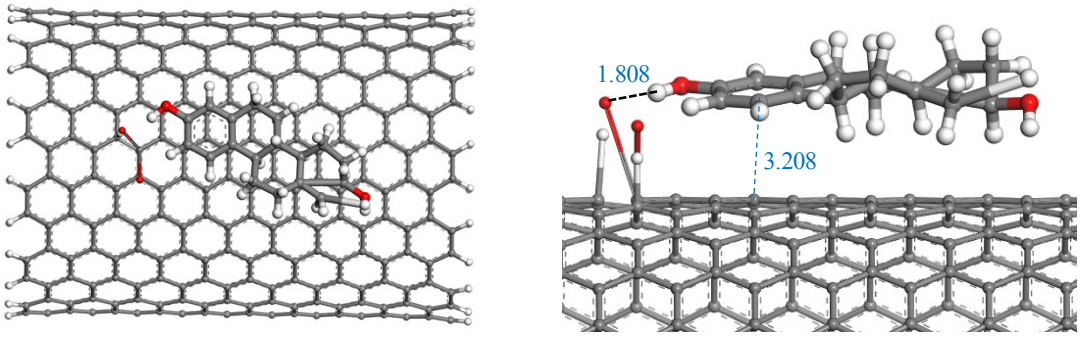

(e) CNTs-COO$^-$ + EE2

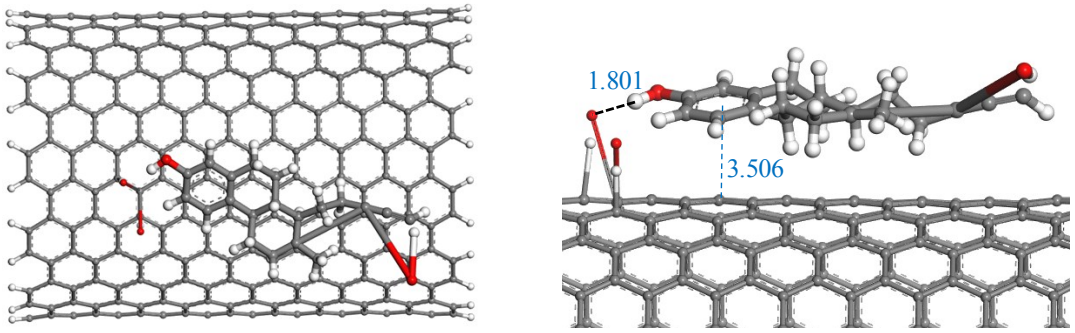

(f) GO + E2

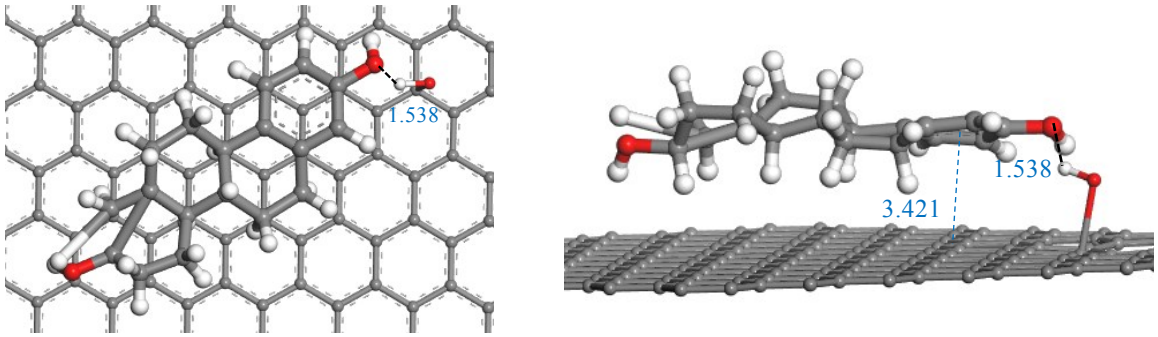

(g) GO + EE2

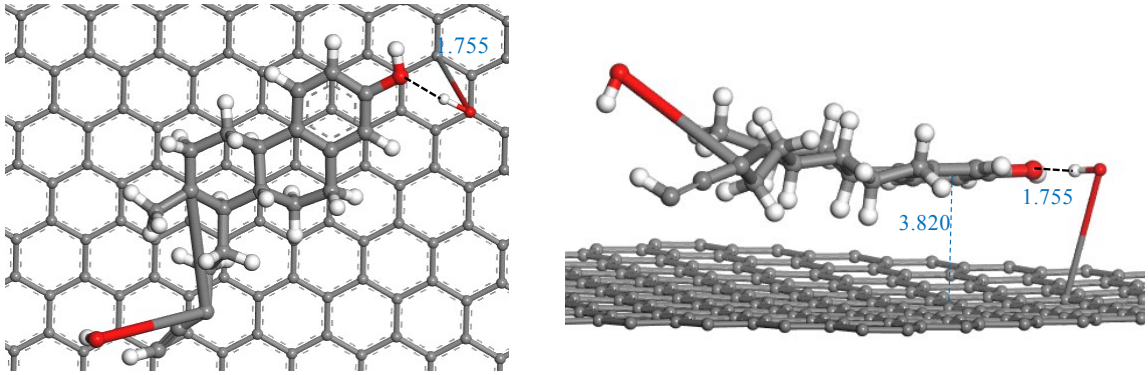

C O H

Fig. S10 DFT-optimized geometries for carboxylated CNTs and GO (a and b), E2 or EE2 in solution (c) and adsorbed to CNTs and GO (d-g).

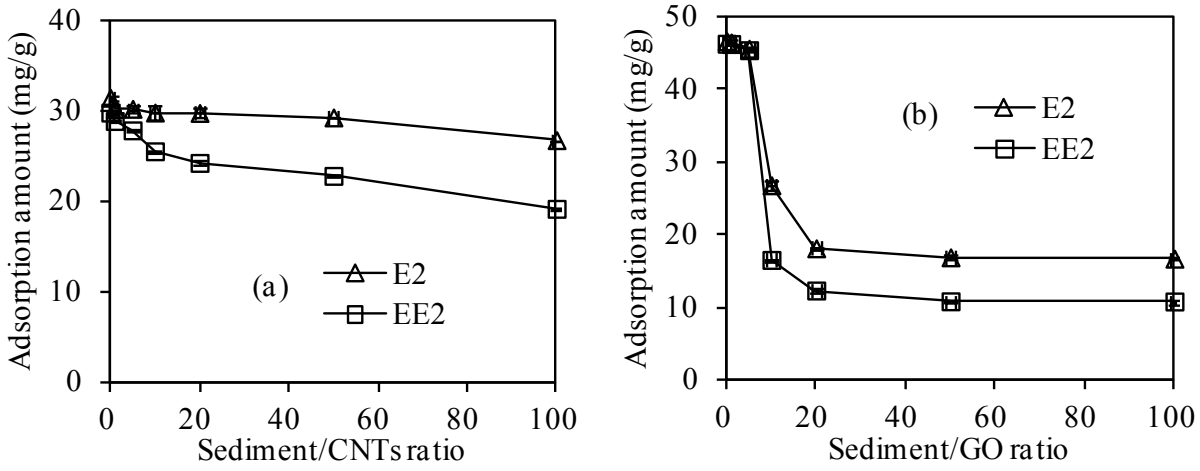

219

220 **Fig. S11** Adsorption of E2 and EE2 to CNTs (a) and GO (b) in presence of sediments at various

221 sediment/CNM ratios (CNMs concentration = 50 mg/L, initial concentration of E2 or EE2 = 2.40

222 mg/L, and sediment particle size < 63 μm).

223

224

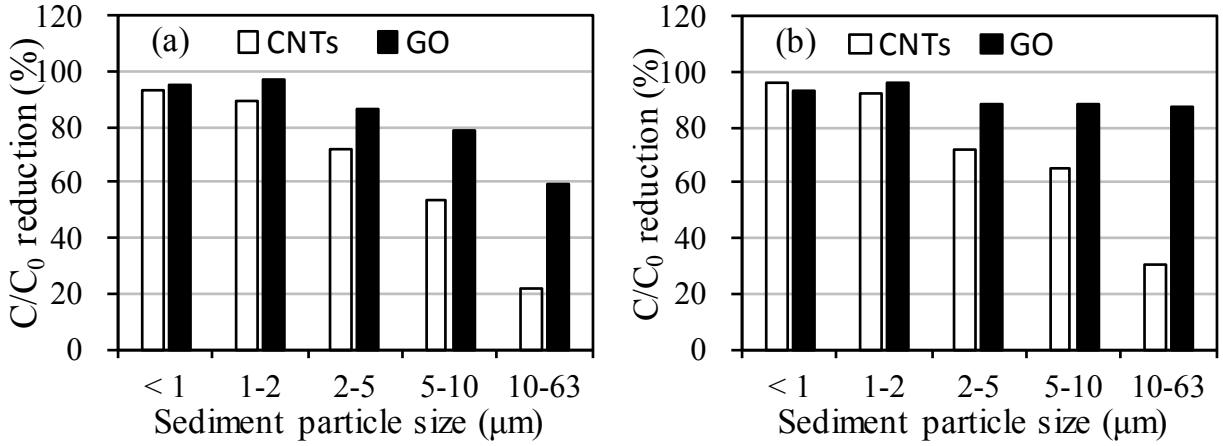

225

226 **Fig. S12** C/C_0 reduction in presence of various sediment size fractions: (a) untreated sediments

227 and (b) OM-free sediments.

228

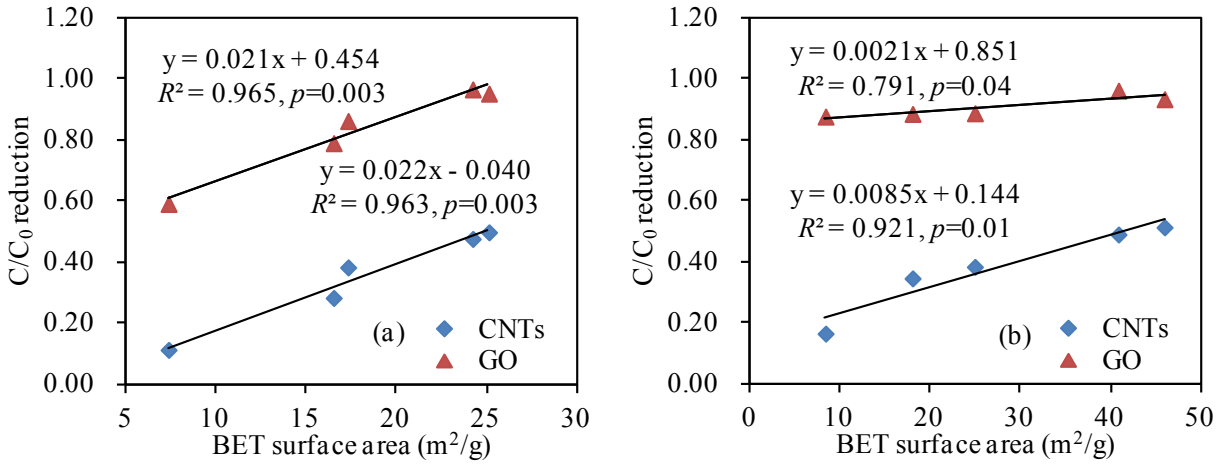

229

230 **Fig. S13** The relationship between C/C_0 reduction and BET surface areas of sediments (a) and

231 OM-free sediments (b).

232

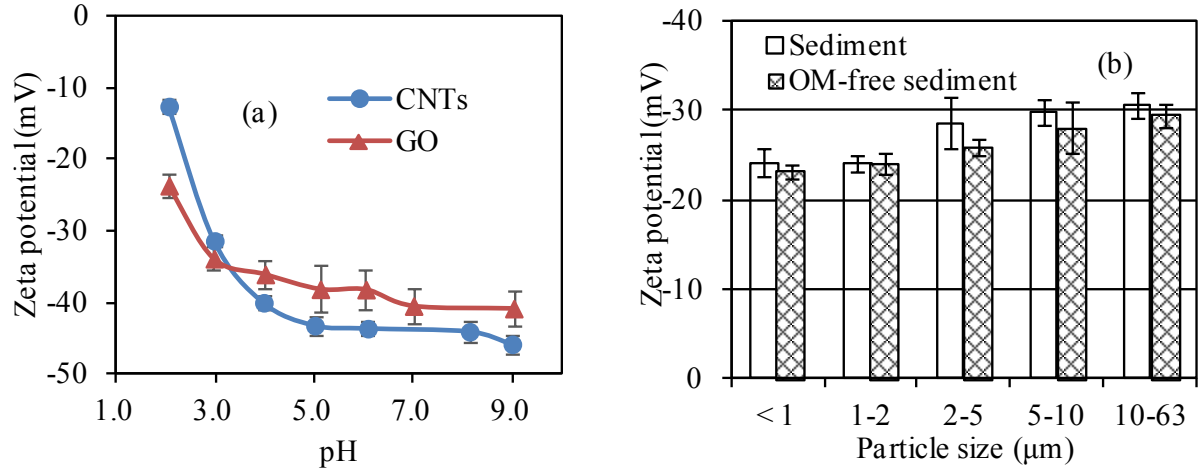

233

234 **Fig. S14** Zeta potentials of CNMs (a) and various sediment size fractions (b).

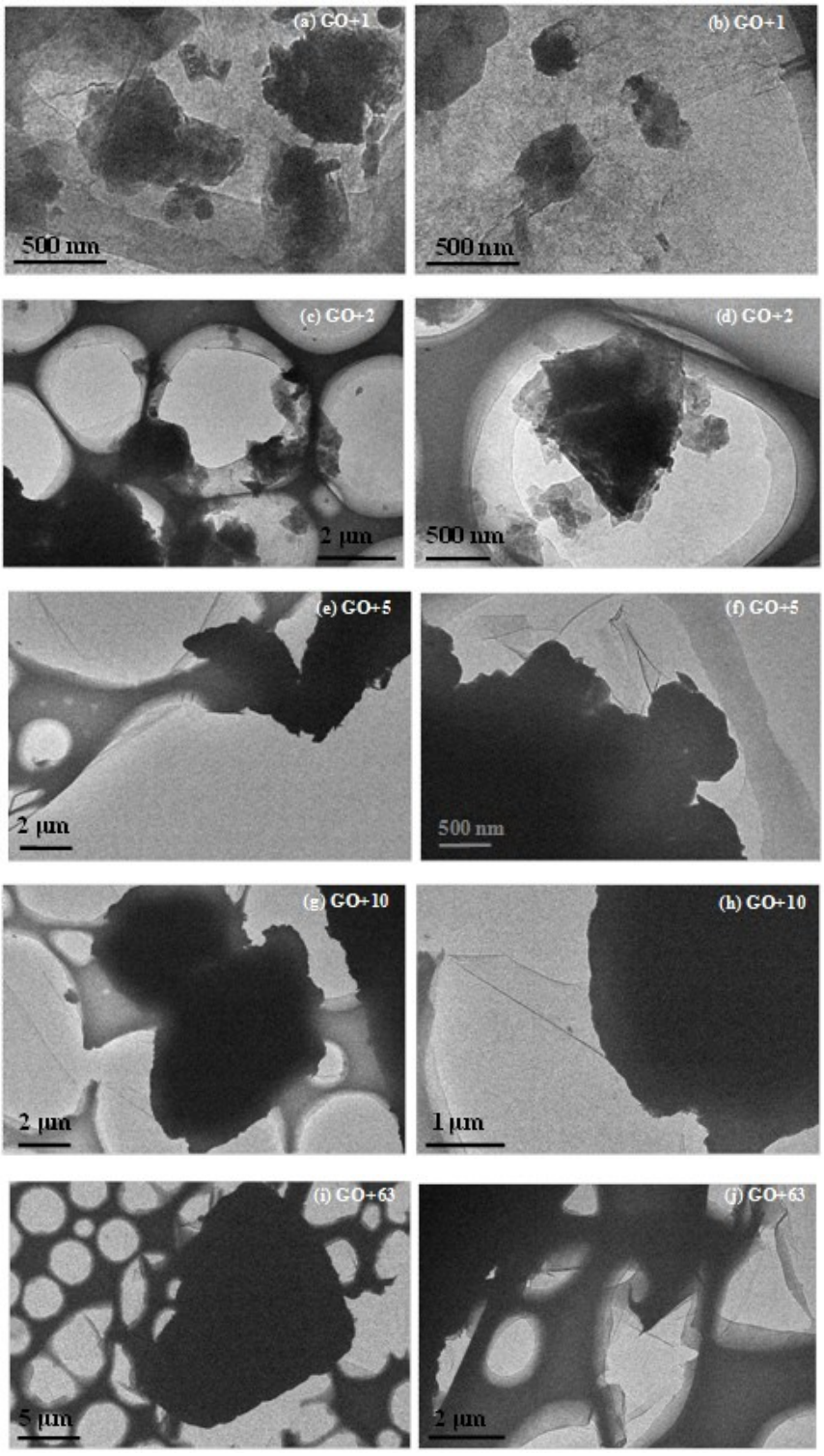

Fig. S15 TEM images of GO mixtures with various sediment size fractions (GO = 50 mg/L, sediment/GO = 10).

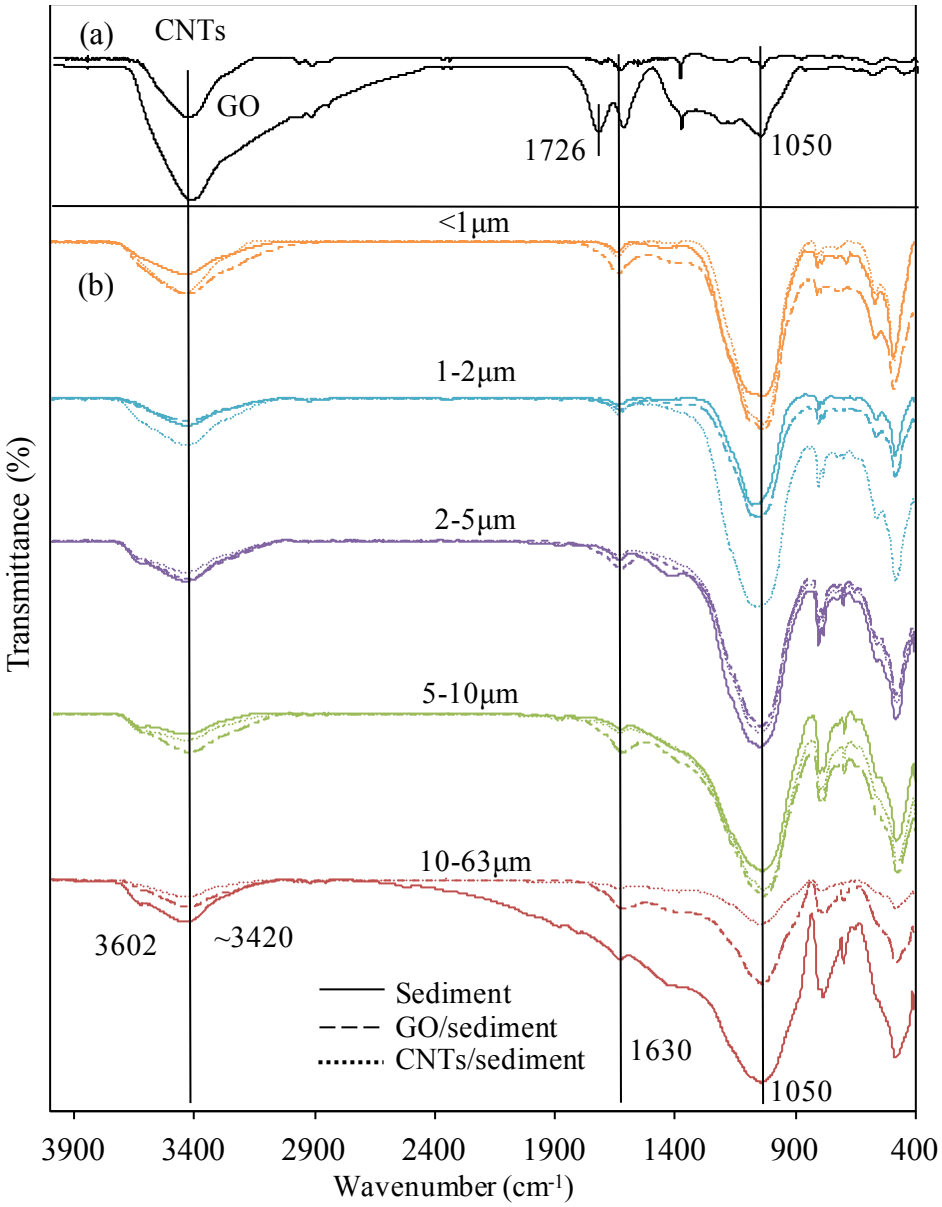

242

243 **Fig. S16** FTIR spectra of CNTs and GO (a), OM-free sediments and their mixtures with CNMs

244 (b).

245

246

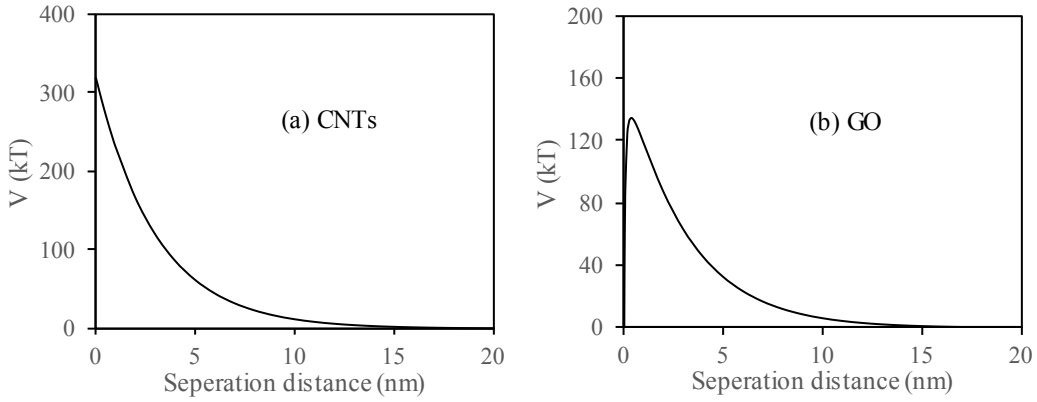

247

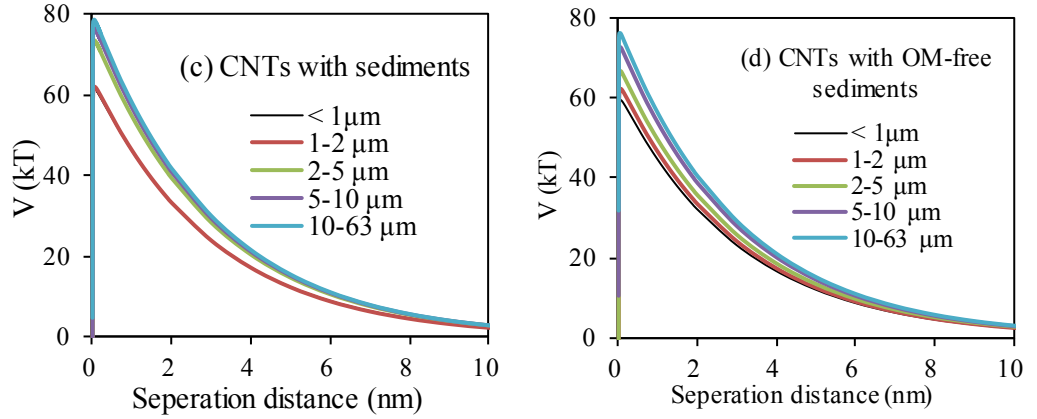

248

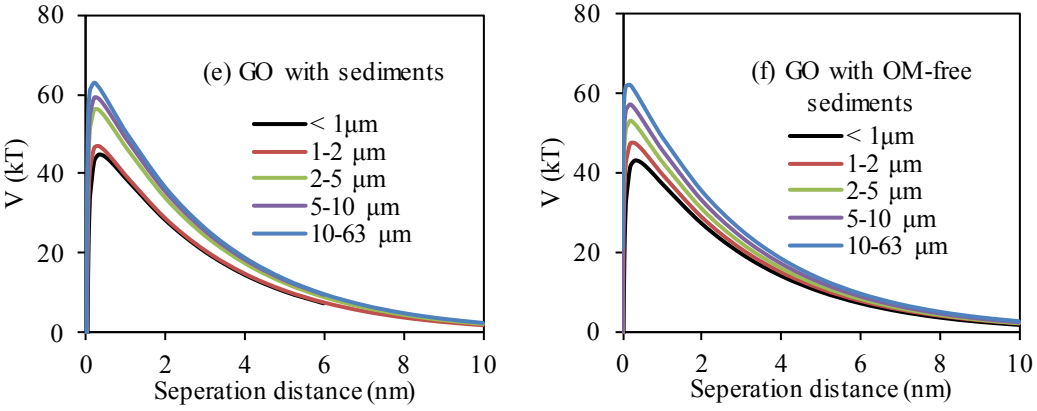

249 **Fig. S17** Interaction energies between CNTs (a) or GO (b), and CNMs with sediments (c and e) or

250 OM-free sediments (d and f) calculated by the DLVO theory.

251

References

S1 J. H. Dane and G. C. Topp, Soil Science Society of America, Madison, WI, 2002.

S2 W. L. Sun and K. Zhou, *Chem. Eng. J.*, 2014, 258, 185-193.

S3 W. L. Sun, C. S. Zhang, N. Xu and J. R. Ni, *Environ. Pollut.*, 2015, 205, 111-120.

S4 J. M. Wei, W. L. Sun, W. Y. Pan, X. Q. Yu, G. Sun and H. Jiang, *Chem. Eng. J.*, 2017, 312, 167-179.

S5 J. Zhou, H. Li, J. Lu, G. F. Luo, L. Lai, R. Qin, L. Wang, S. Nagase, Z. X. Gao, W. Mei, G. P. Li, D. P. Yu and S. Sanvito, *Nano Res.*, 2010, 3, 296-306.

S6 J. M. Zheng, Z. Y. Ren, P. Guo, L. Fang and J. Fan, *Appl. Surf. Sci.*, 2011, 258, 1651-1655.

S7 P. Verma, J. Weir, L. Mirica and T. D. Stack, *Inorg. Chem.*, 2011, 50, 9816-9825.

S8 L. M. Wu, J. Xiao, Y. Wu, S. K. Xian, G. Miao, H. H. Wang, Z. Li, *Langmuir*, 2014, 30, 1080-1088.

S9 M. Elimelech, J. Gregory and X. Jia, Butterworth-Heinemann Ltd, Oxford, MA, 2013.

S10 Y. Tian, B. Gao, C. Silvera-Batista, K. J. Ziegler, *J. Nanopart. Res.*, 2010, 12, 2371-2380.

S11 Y. Wang, B. Gao, V. L. Morales, Y. Tian, L. Wu, J. Gao, W. Bao, L. Y. Yang, *J. Nanopart. Res.*, 2012, 14, 1-9.

S12 J. Bergendahl and D. Grasso, *AIChE J.*, 1999, 45, 475-484.

S13 K.L. Chen and M. Elimelech, *J. Colloid Interface Sci.*, 2007, 309, 126-134.

S14 J. N. Israelachvili, Academic press, 2011.

S15 I. Chowdhury, M. C. Duch, N. D. Mansukhani, M. C. Hersam and D. Bouchard, *Environ. Sci. Technol.*, 2013, 47, 6288-6296.

S16 D. B. Hough and L. R. White, *Adv. Colloid Interface Sci.*, 1980, 14, 3-41.

S17 W. Liu, W. Sun, A. G. L. Borthwick and J. R. Ni, *Colloids Surface A*, 2013, 434, 319-328.